BLM helicase regulates DNA repair by counteracting RAD51 loading at DNA double-strand break sites

Dharm S. Patel, Sarah M. Misenko, Joonyoung Her, and Samuel F. Bunting

Department of Molecular Biology and Biochemistry, Rutgers, The State University of New Jersey, Piscataway, NJ

The *BLM* gene product, BLM, is a RECQ helicase that is involved in DNA replication and repair of DNA double-strand breaks by the homologous recombination (HR) pathway. During HR, BLM has both pro- and anti-recombinogenic activities, either of which may contribute to maintenance of genomic integrity. We find that in cells expressing a mutant version of BRCA1, an essential HR factor, ablation of *BLM* rescues genomic integrity and cell survival in the presence of DNA double-strand breaks. Improved genomic integrity in these cells is linked to a substantial increase in the stability of RAD51 at DNA double-strand break sites and in the overall efficiency of HR. Ablation of *BLM* also rescues RAD51 foci and HR in cells lacking BRCA2 or XRCC2. These results indicate that the anti-recombinase activity of BLM is of general importance for normal retention of RAD51 at DNA break sites and regulation of HR.

Introduction

Individuals with biallelic mutations in the *BLM* gene are affected by Bloom syndrome (BS), a heritable condition associated with developmental abnormalities and susceptibility to a range of malignancies at an early age (Ellis et al., 1995). The *BLM* gene product is a helicase of the RECQ family with roles in DNA replication and repair. BLM protein acts at several steps of the homologous recombination (HR) pathway for DNA double-strand break (DSB) repair (Larsen and Hickson, 2013). First, BLM, along with the endonuclease Dna2, contributes to resection of DNA DSBs to generate a single-stranded intermediate that is bound by replication protein A (RPA) and RAD51 (Gravel et al., 2008; Nimonkar et al., 2008, 2011). The RAD51 nucleoprotein filament then pairs with matching sequence in a homologous DNA template, leading to strand invasion and creation of a "D-loop" structure. This process can be inhibited by BLM, representing a potential anti-recombinogenic effect of the protein (van Brabant et al., 2000; Hu et al., 2001; Wu and Hickson, 2003; Bachrati et al., 2006; Bugreev et al., 2007). After resynthesis of DNA across the break site, BLM resolves heteroduplex recombination intermediates by dissolving Holliday junctions, restoring separate DNA duplexes (Wu and Hickson, 2003). The ability of BLM to dissolve Holliday junctions limits the frequency of genetic exchanges between homologous sequences during HR. This is consistent with a marked increase in sister chromatid exchanges (SCEs) in BS cells (Chaganti et al., 1974; Hu et al., 2001).

The ability of BLM to limit crossover resolution of HR intermediates has been suggested to represent its key activity in limiting genomic instability (Luo et al., 2000). According to this model, the absence of BLM leads to an excessive number of loss-of-heterozygosity events owing to increased crossover recombination, which leads to malignancy. BS cells also show an increase in chromosome breaks and rearrangements, potentially indicating that BLM provides one or more additional repair activities (Chu et al., 2010). This activity may be related to the pro-recombinogenic role of BLM during DSB resection or an anti-recombinogenic effect around the time of D-loop formation.

In this study, we use a genetic approach to test whether pro- or anti-recombinogenic activities of BLM are most relevant for maintenance of genomic integrity in mammalian cells. We find that BLM contributes significantly to genomic instability in cells in which key HR factors are missing, suggesting that the anti-recombinogenic role of BLM has the potential to exert a significant influence on the efficiency of HR in cancer cells. BLM appears to exert this effect by displacing RAD51 from resected DNA intermediates in a process that is dependent on BLM helicase activity but does not require association with DNA topoisomerase IIIα.

Results

Ablation of *Blm* rescues genomic instability and cell survival in *Brca1*$^{\Delta 11/\Delta 11}$ cells

BLM has been shown to act with the endonuclease Dna2 to promote formation of 3′ single-stranded overhangs at DSB sites (Gravel et al., 2008; Nimonkar et al., 2008, 2011). This process contributes to the efficiency of HR; however, the exonuclease Exo1 can perform a similar function in mammalian cells. To

Correspondence to Samuel F. Bunting: bunting@cabm.rutgers.edu

Abbreviations used: BS, Bloom syndrome; CSR, class switch recombination; DSB, double-strand break; HR, homologous recombination; IR, ionizing radiation; IRIF, ionizing radiation–induced foci; MEF, mouse embryonic fibroblast; NHEJ, nonhomologous end joining; RPA, replication protein A; SCE, sister chromatid exchange.

The Rockefeller University Press
J. Cell Biol. Vol. 216 No. 11 3521–3534
https://doi.org/10.1083/jcb.201703144

evaluate the importance of BLM in generating 3′ single-stranded regions at DSBs, we used mice with conditional deletion of *Blm* in the B lymphocyte lineage, crossed to *Trp53bp1*$^{-/-}$ mice (Fig. 1, A and B; and Fig. S1 A; Rickert et al., 1997; Ward et al., 2004; Chester et al., 2006). *Blm*$^{\Delta/\Delta}$ cells showed an increased frequency of chromosome aberrations after exposure to either olaparib or mitomycin C, which induce DSBs in dividing cells. *Trp53bp1*$^{-/-}$ mice lack 53BP1, a negative regulator of DSB resection (Bunting et al., 2010; Chapman et al., 2012; Hakim et al., 2012). We reasoned that increased formation of 3′ single-stranded overhangs at DSBs in *Trp53bp1*$^{-/-}$ mice might rescue genomic instability arising from loss of the DSB resection activity of BLM. *Blm*$^{\Delta/\Delta}$;*Trp53bp1*$^{-/-}$ cells showed chromosome instability equivalent to *Blm*$^{\Delta/\Delta}$;*Trp53bp1*$^{+/+}$ cells, indicating that removing a barrier to resection is not sufficient to substitute for BLM in the early stages of HR. On the other hand, *Brca1*$^{\Delta11/\Delta11}$;*Blm*$^{\Delta/\Delta}$ cells showed a frequency of chromosome aberrations that was significantly lower than that seen in *Brca1*$^{\Delta11/\Delta11}$ cells (Fig. 1, A and B; and Fig. S1, A and B). *Brca1*$^{\Delta11/\Delta11}$ cells normally have a high level of genomic instability that arises at least in part because of a failure to perform HR (Moynahan et al., 1999; Xu et al., 1999; Bunting et al., 2010). This genomic instability is dependent on the presence of BLM, indicating that BLM contributes to the defect in HR in *Brca1*$^{\Delta11/\Delta11}$ cells.

We used two assays to test whether the different levels of genomic instability in *Brca1*$^{\Delta11/\Delta11}$, *Blm*$^{\Delta/\Delta}$, and *Brca1*$^{\Delta11/\Delta11}$;*Blm*$^{\Delta/\Delta}$ cells affected their ability to divide and proliferate. First, we targeted *Brca1* in the thymus using a conditional knockout approach to produce *Brca1*$^{\Delta11/\Delta11}$ thymocytes (Hennet et al., 1995). These *Brca1*$^{\Delta11/\Delta11}$ thymocytes show a partial developmental block at the transition from the CD4$^-$ CD8$^-$ "double negative" stage to the CD4$^+$ CD8$^+$ "double positive" stage, corresponding to apoptosis induced by genomic instability (Fig. 1, C and D; Mak et al., 2000). In contrast, *Brca1*$^{\Delta11/\Delta11}$;*Blm*$^{\Delta/\Delta}$ cells showed a significantly reduced block at the double-negative to double-positive transition. The improved DNA repair seen in *Brca1*$^{\Delta11/\Delta11}$;*Blm*$^{\Delta/\Delta}$ cells relative to *Brca1*$^{\Delta11/\Delta11}$ cells is therefore relevant in a physiological setting. Second, we used a colony forming assay to measure the ability of WT and *Brca1*$^{\Delta11/\Delta11}$ mouse embryonic fibroblast (MEF) cells to proliferate in vitro after exposure to olaparib (Fig. 1 E). Whereas *Brca1*$^{\Delta11/\Delta11}$ cells stably expressing a control shRNA showed substantial hypersensitivity to olaparib, knockdown of *BLM* afforded a significant rescue of cell survival (Fig. 1 F). BLM therefore contributes to cell death in *Brca1*-deficient cells, in a manner that correlates with improved DSB repair.

Enhanced RAD51 stability at DNA break sites and HR in *Brca1*$^{\Delta11/\Delta11}$ cells after deletion of *Blm*

To understand how BLM impacts DNA repair in *Brca1*$^{\Delta11/\Delta11}$ cells, we measured nuclear ionizing radiation–induced foci (IRIF) of RAD51, which mark sites of HR-mediated DNA repair. *Brca1*$^{\Delta11/\Delta11}$ cells are defective for IRIF of RAD51 (Bhattacharyya et al., 2000; Huber et al., 2001), but we found that the proportion of cells exhibiting RAD51 foci was equivalent to WT in *Brca1*$^{\Delta11/\Delta11}$;*Blm*$^{\Delta/\Delta}$ B cells (Fig. 2, A and B). RAD51 foci were also observed in *Brca1*$^{\Delta11/\Delta11}$ MEFs after shRNA-mediated knockdown of BLM, whereas cells expressing control shRNA showed a defect in RAD51 foci formation (Fig. 2, C–E). BLM therefore appears to limit RAD51 assembly at DSBs in *Brca1*$^{\Delta11/\Delta11}$ cells. Several factors that regulate the assembly and recruitment of RAD51 at break sites have also been shown to regulate RAD51-mediated protection of DNA replication forks (Schlacher et al., 2012; Higgs et al., 2015; Leuzzi et al., 2016; Sato et al., 2016). Using a DNA fiber assay, we found that BLM affected fork protection (Fig. 2, F and G). As previously reported, *Brca1*$^{\Delta11/\Delta11}$ cells show a defect in fork protection relative to WT cells after hydroxyurea treatment (Ray Chaudhuri et al., 2016). Deletion of *Blm* in *Brca1*$^{\Delta11/\Delta11}$ cells afforded a partial rescue of fork degradation, which may be related to the ability of BLM to regulate the stability of RAD51 at nascent replication tracts after replication stress.

Next, we used U2OS EJ-DR reporter cells to directly measure the importance of BLM for HR efficiency after siRNA-mediated silencing of *BLM* and *BRCA1* (Fig. 3, A and B; Bindra et al., 2013). Consistent with previous studies and our RAD51 foci results (Fig. 2, A–E), we observed that the rate of HR was substantially reduced in cells expressing BRCA1$^{\Delta11}$. The rate of HR showed a highly significant increase upon codepletion of BLM, however, to a level equivalent to that seen in control cells (Fig. 3 C). Rates of nonhomologous end joining (NHEJ) were not significantly different in any of the conditions tested (Fig. 3 D). The differences in cell viability and genomic instability between *Brca1*$^{\Delta11/\Delta11}$ and *Brca1*$^{\Delta11/\Delta11}$;*Blm*$^{\Delta/\Delta}$ cells are therefore correlated with the efficiency of HR.

As a second measure of HR, we assayed the frequency of SCEs, which are formed through crossover HR, in *Brca1*$^{\Delta11/\Delta11}$, *Blm*$^{\Delta/\Delta}$, and *Brca1*$^{\Delta11/\Delta11}$;*Blm*$^{\Delta/\Delta}$ metaphase chromosome spreads (Fig. S2, A and B). Whereas WT and *Brca1*$^{\Delta11/\Delta11}$ cells showed an approximately equivalent frequency of SCEs, *Blm*$^{\Delta/\Delta}$ cells showed an elevated rate of SCEs, consistent with the known role of BLM in promoting noncrossover resolution of Holliday junctions during the final stages of HR (Chaganti et al., 1974; Wu and Hickson, 2003). *Brca1*$^{\Delta11/\Delta11}$;*Blm*$^{\Delta/\Delta}$ chromosomes had fewer SCEs than the high rate seen in *Blm*$^{\Delta/\Delta}$ cells, but the rate was nonetheless equivalent to or higher than that seen in WT cells.

BLM modifies HR activity in WT cells, but not BRCA1-nullizygous cells

The *Brca1*$^{\Delta11}$ allele is considered to be hypomorphic (Evers and Jonkers, 2006); hence, we sought to test whether the observed anti-recombinase activity of BLM is also relevant in other BRCA1 mutant cells or in WT cells. Although silencing *Blm* rescues HR in *Brca1*$^{\Delta11/\Delta11}$ cells, we found that the extent of rescue of RAD51 foci formation was insubstantial in MDA-MB-436 (Elstrodt et al., 2006), a human mammary adenocarcinoma cell line that expresses no BRCA1 protein (Fig. 4, A and B). We also failed to observe rescue of RAD51 foci formation in U2OS osteosarcoma cells after cosilencing of *BRCA1* and *BLM* using siRNA (Fig. 4, C and D; and Fig. S2 C). Silencing of *BLM* likewise failed to rescue the HR defect of U2OS EJ-DR reporter cells in which *BRCA1* was knocked down (Fig. 4 E). Some residual pro-recombinogenic activity provided by the hypomorphic BRCA1$^{\Delta11}$ protein that is expressed in *Brca1*$^{\Delta11/\Delta11}$ cells is therefore necessary for HR even in the absence of *Blm*. BLM appears to regulate the efficiency of HR, and loss of BLM cannot completely substitute for essential HR factors.

An anti-recombinogenic activity of BLM has previously been inferred from the high rate of SCEs in BS cells (Chaganti et al., 1974; Hu et al., 2001). Using the EJ-DR reporter assay, we tested whether overexpression of BLM could suppress HR in *BLM*$^{+/+}$ cells. As has been seen with other mammalian

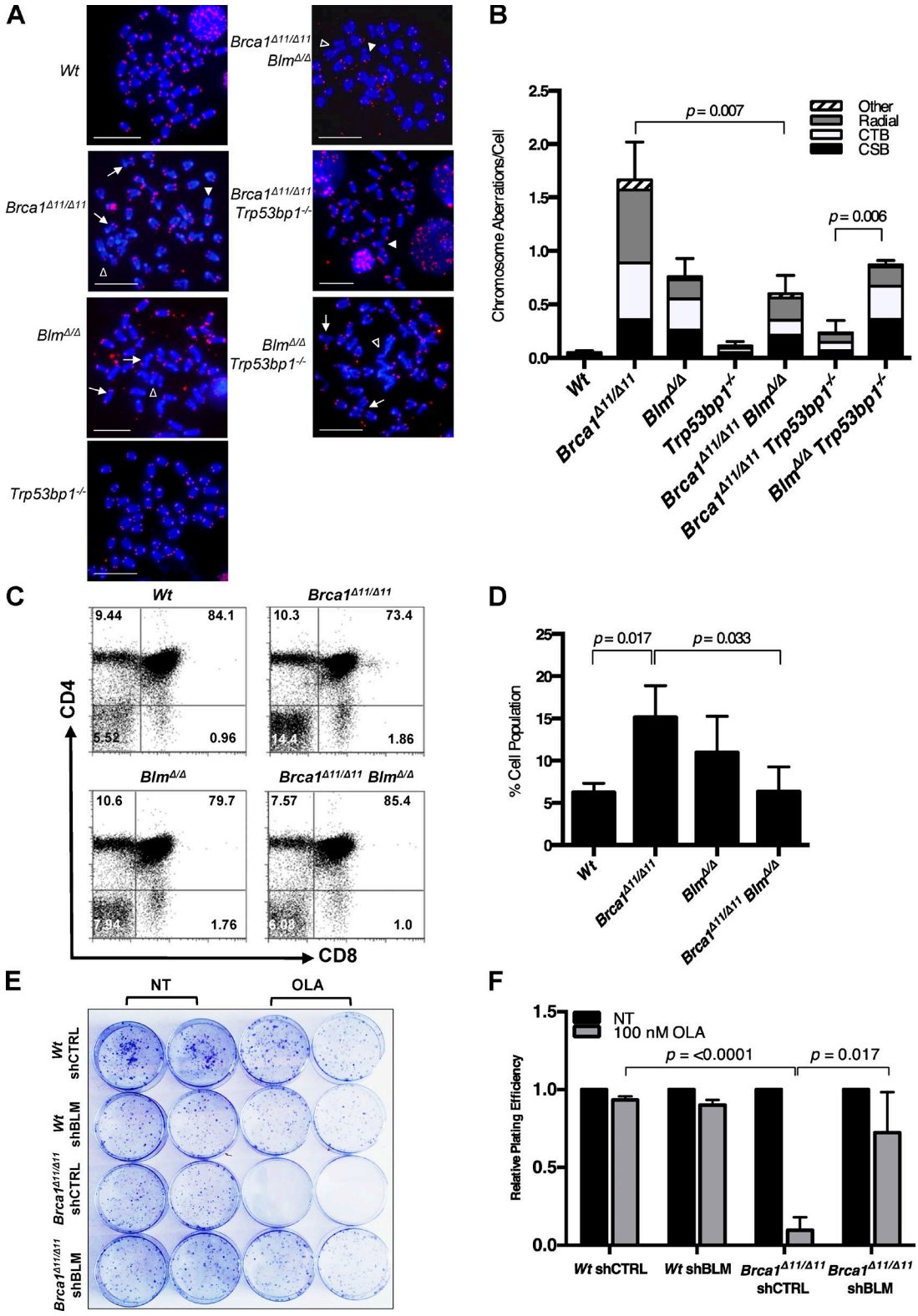

Figure 1. **Ablation of *Blm* rescues genomic instability, T cell development, and poly (ADP-ribose) polymerase inhibitor sensitivity in *Brca1*$^{\Delta 11/\Delta 11}$ cells.** (A) Metaphase spreads from primary mouse B lymphocyte cells stained with DAPI and Cy3-labeled telomeric probe. The arrows point to chromatid breaks, closed arrowheads point to chromosome breaks, and open arrowheads point to radial chromosomes. Bars, 10 µm. (B) Quantification of genomic instability in metaphase spreads after 2 µM overnight treatment with the poly (ADP-ribose) polymerase inhibitor olaparib. CSB, chromosome breaks; CTB, chromatid breaks. (C) Flow cytometry data from primary T lymphocyte cells from mice of indicated genotypes stained with CD4 and CD8 antibodies. (D) Quantification of $CD4^{-}$ $CD8^{-}$ double-negative T cells. (E) Clonogenic survival assay after BLM knockdown in WT and BRCA1$^{\Delta 11/\Delta 11}$ cells with no treatment (NT) and chronic treatment with 100 nM Olaparib (OLA), a poly (ADP-ribose) polymerase inhibitor. (F) Quantification of clonogenic survival assay after shBLM in WT and BRCA1$^{\Delta 11/\Delta 11}$ MEFs. Graphs represent mean ± SD of three independent experiments.

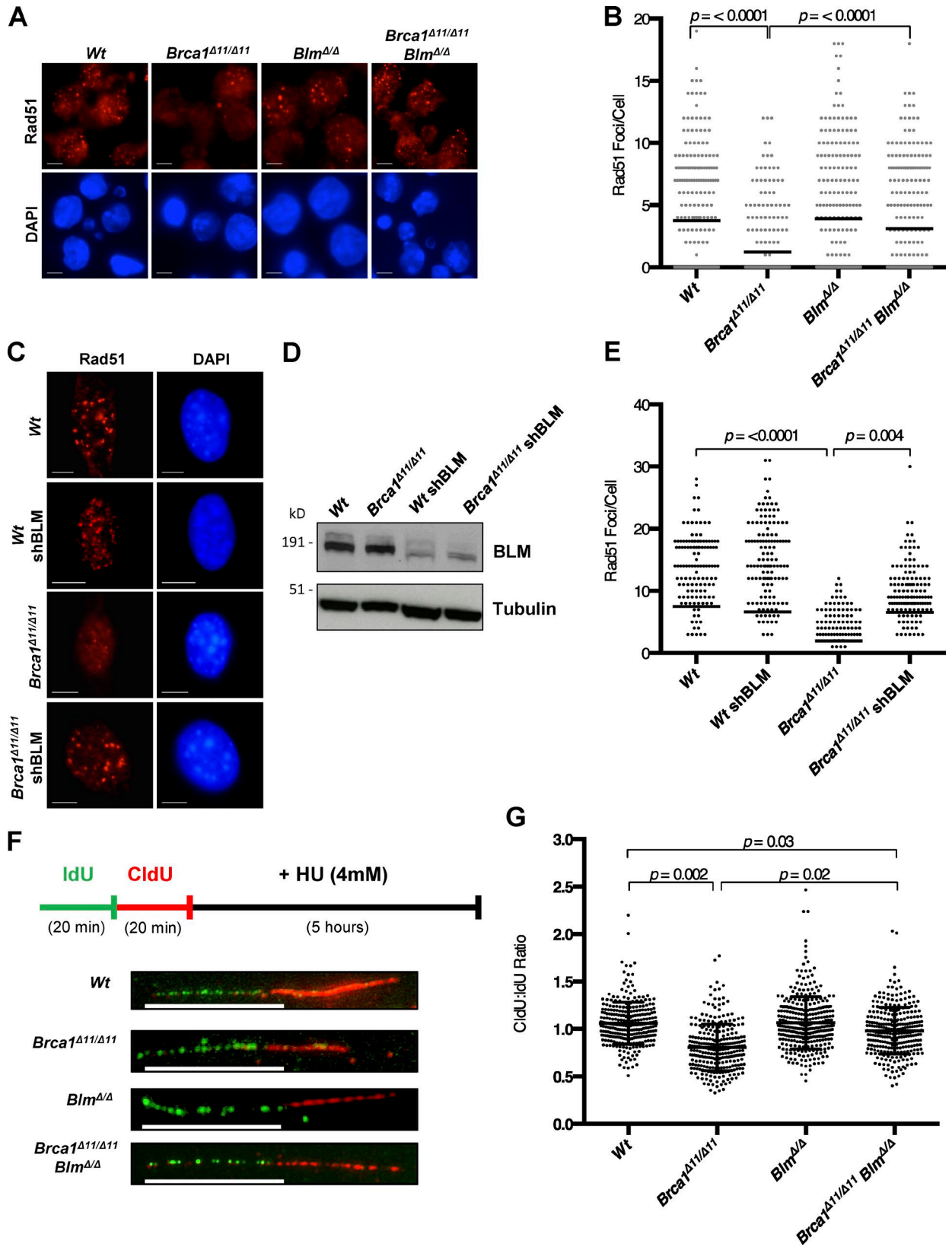

Figure 2. **Enhanced Rad51 foci after ablation of *Blm* in *Brca1*$^{\Delta 11/\Delta 11}$ cells.** (A) Immunofluorescence analysis of Rad51 IRIF in primary B cells from mice of indicated genotypes after IR. (B) Quantification of Rad51 IRIF in primary B cells. (C) Immunofluorescence analysis of Rad51 IRIF in MEF cells with indicated genotypes and shRNA knockdown after IR. (D) Western blot analysis of knockdown efficiency. (E) Quantification of Rad51 IRIF in MEF cells. (F) Experimental scheme and representative images of replication fork degradation analysis after 20 min iododeoxyuridine (IdU) and chlorodeoxyuridine (CldU) labeling, respectively, and exposure to 4 mM hydroxyurea (HU) for 5 h. (G) DNA fiber analysis denoting the mean ratios of CldU/IdU label lengths. Graphs represent mean ± SD of three independent experiments. Bars, 10 µm.

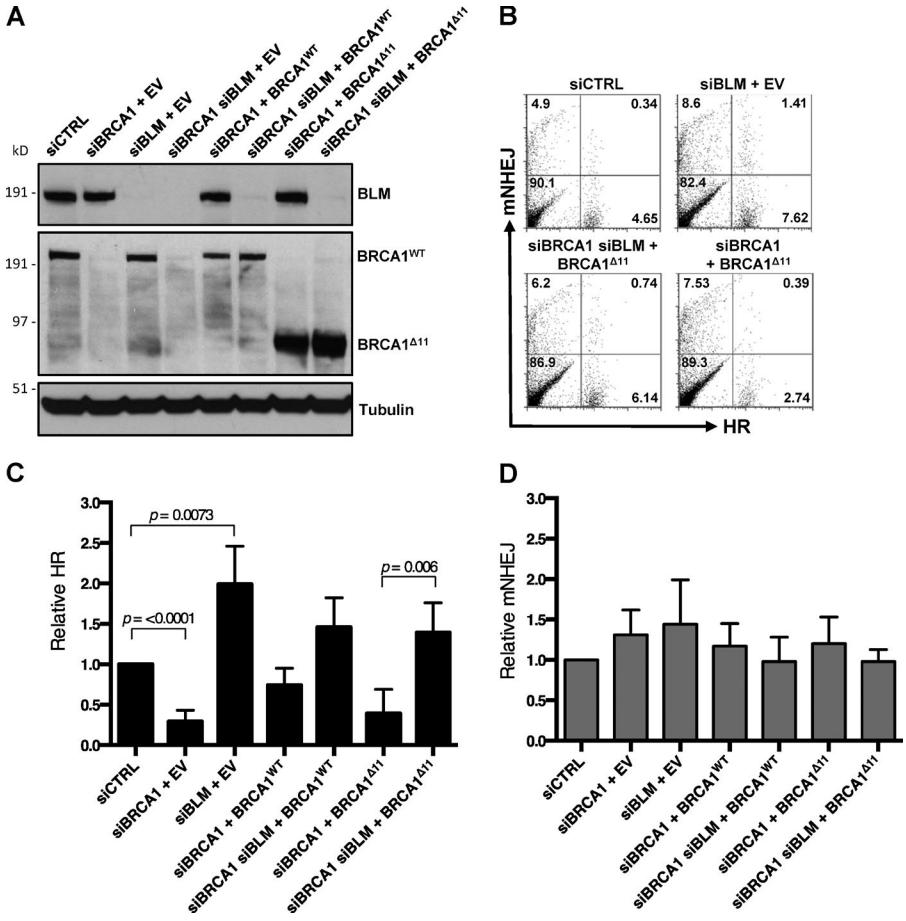

Figure 3. **BLM regulates HR in BRCA1$^{\Delta 11}$ cells.** (A) Western blot analysis of EJ-DR reporter cells transfected with siRNA oligos and/or BRCA1 expression vector or control empty vector (EV). (B) Representative flow cytometry data in the U2OS EJ-DR reporter assay, in which HR-mediated repair of I-SceI–mediated DSBs produces GFP fluorescence and mutagenic NHEJ (mNHEJ) produces DsRed fluorescence. (C) Analysis of relative HR frequency in the U2OS EJ-DR reporter cell line. (D) Analysis of relative mNHEJ frequency in the U2OS EJ-DR reporter cell line. Graphs represent mean ± SD of three independent experiments.

anti-recombinases (Fugger et al., 2009; Lorenz et al., 2009; Schwendener et al., 2010), overexpression of BLM caused a modest but statistically significant reduction in HR efficiency (Figs. 4 F and S2 D). Suppression of HR was not observed, however, upon overexpression of a helicase-dead BLM mutant (BLM^{K695A}; Bugreev et al., 2007). BLM therefore has the potential to disrupt HR in WT and *Brca1*$^{\Delta 11/\Delta 11}$ cells through its helicase activity. The ability of BLM to dissolve Holliday junctions is further dependent on formation of the multiprotein BTR complex (BLM–topoisomerase III-α–RMI1/2; Manthei and Keck, 2013). To test whether BTR is required for BLM anti-recombinase activity, we measured HR efficiency in cells after siRNA-mediated silencing of *BRCA1* and topoisomerase IIIα (*TOP3A*). In cells expressing mutant BRCA1$^{\Delta 11}$, silencing *TOP3A* did not rescue the low efficiency of HR (Fig. 5 A). The anti-recombinase effect of BLM that is active in this assay therefore appears to be independent of the BTR complex. This represents a difference from BLM-mediated dissolution of Holliday junctions, which is dependent on the BTR complex (Wu and Hickson, 2003). NHEJ was not defective in any of the cells tested upon depletion of BLM or TOP3A (Fig. 5 B).

The presence of 53BP1 at DSB sites regulates the efficiency of DSB resection and entry into the HR pathway (Chapman et al., 2012). 53BP1 limits DSB resection and increases the proportion of DSBs that are repaired by NHEJ. We hypothesized that the different levels of repair seen in *Brca1*$^{\Delta 11/\Delta 11}$ and *Brca1*$^{\Delta 11/\Delta 11}$*;Blm*$^{\Delta/\Delta}$ cells may be related to differential 53BP1 recruitment to DSB sites in these cells. We therefore measured the number of 53BP1 foci formed after ionizing radiation (IR) treatment (Fig. 5 C). Deletion of *Blm* was associated with a slight reduction in 53BP1 foci formation relative to WT, as has been reported previously (Grabarz et al., 2013). However, *Brca1*$^{\Delta 11/\Delta 11}$*;Blm*$^{\Delta/\Delta}$ cells showed a significantly greater number of 53BP1 foci after IR compared with *Blm*$^{\Delta/\Delta}$ cells (Fig. 5, C and D). As the difference in 53BP1 foci was not of great magnitude, we measured class switch recombination (CSR), which is highly sensitive to 53BP1 levels (Manis et al., 2004; Ward et al., 2004). Although *Brca1*$^{\Delta 11/\Delta 11}$ and *Blm*$^{\Delta/\Delta}$ cells did not show substantial differences in CSR, the rate of switching was markedly reduced in *Trp53bp1*$^{-/-}$ cells (Fig. S3, A and B). Interestingly, the increased accumulation of 53BP1 in *Brca1*$^{\Delta 11/\Delta 11}$*;Blm*$^{\Delta/\Delta}$ B cells relative to *Brca1*$^{\Delta 11/\Delta 11}$ cells was sufficient to impact the efficiency of CSR. On the other hand, we did not observe any substantial defects in the accumulation of RPA at sites of IR–induced damage in any of the genotypes used (Fig. 5, E and F; and Fig. S3, C and D). These results show that although deletion of *Brca1* or *Blm* can impact 53BP1 recruitment, this effect does not substantially alter DSB resection, as revealed by RPA accumulation. The difference in HR efficiency between *Brca1*$^{\Delta 11/\Delta 11}$ and *Brca1*$^{\Delta 11/\Delta 11}$*;Blm*$^{\Delta/\Delta}$ cells is therefore likely to be dependent on a subsequent step in the HR pathway, when RAD51 is loaded.

Rescue of RAD51 foci formation and HR in BRCA2- and XRCC2-deficient cells by silencing of *BLM*

Efficient HR is dependent on several factors that contribute to accumulation of RAD51 at resected DSBs. These include PALB2 (partner and localizer of BRCA2), BRCA2, and XRCC2 (Johnson et al., 1999; O'Regan et al., 2001; Xia et al., 2006; Jensen et al., 2010). To further dissect the mechanism by

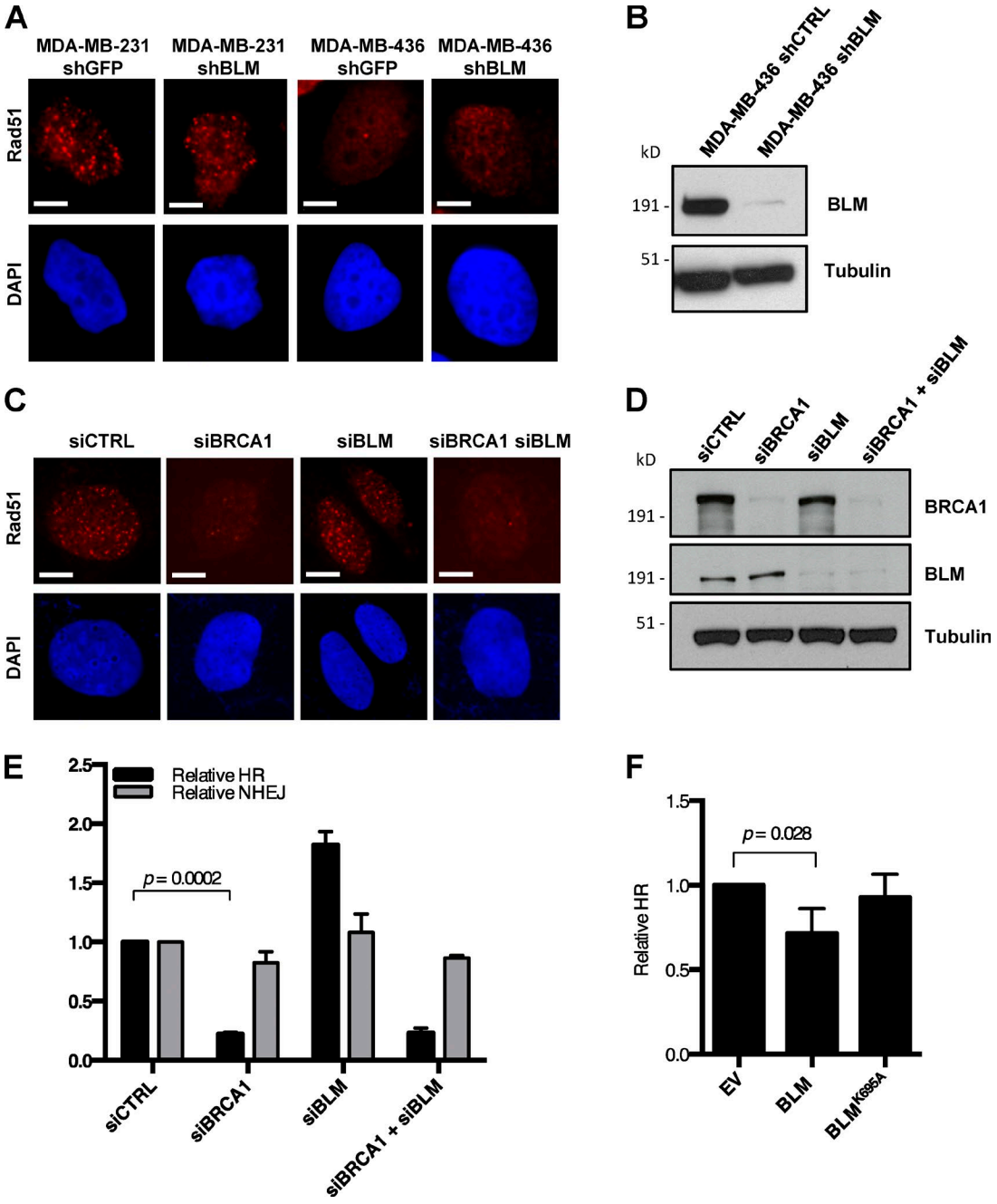

Figure 4. **BLM modifies HR activity in WT cells, but not BRCA1-nullizygous cells.** (A) Immunofluorescence analysis of Rad51 IRIF in MDA-MB-231 (BRCA1 wt) and MDA-MB-436 (BRCA1 mutant) cells after control shRNA or shBLM knockdown. (B) Western blot analysis of BLM knockdown efficiency in MDA-MB-436 cells. (C) Immunofluorescence analysis of Rad51 IRIF in U2OS cells with indicated siRNA knockdown. (D) Western blot analysis of BRCA1 and BLM knockdown efficiency in U2OS cells. (E) Analysis of relative HR and mutagenic NHEJ (mNHEJ) frequency in the EJ-DR U2OS reporter cell line with indicated siRNA knockdown. (F) Analysis of relative HR frequency in the EJ-DR U2OS reporter cell line after overexpression of WT BLM and helicase-dead BLM (BLM^{K695A}). Graphs represent mean ± SD of three independent experiments. Bars, 10 µm.

which BLM coordinates HR, we knocked down each of these factors individually, and in combination with siBLM oligonucleotides (Fig. S4, A–C). Interestingly, ablation of *BLM* was sufficient to rescue RAD51 foci formation in cells treated with either siBRCA2 or siXRCC2 oligos (Fig. 6 A). This result suggests that BLM has a general role in reversing RAD51 nucleoprotein filament formation, which can be revealed in cells lacking key HR factors. Loss of RAD51 foci in siPALB2 cells was not rescued by ablation of *BLM*, suggesting that PALB2 may have a distinct role in RAD51 recruitment. To validate the importance of BLM depletion after silencing of *BRCA2* or *XRCC2*, we used EJ-DR cells to measure HR efficiency. Consistent with the immunofluorescence measurements of RAD51 foci, HR was rescued in both siBRCA2 and siXRCC2 cells after codepletion of BLM (Fig. 6 B).

In separate experiments, we found that knockdown of *TOP3A* did not afford a similar rescue phenotype as was seen with siBLM (Fig. 6, C and D), again suggesting that the ability of BLM to regulate RAD51 stability is likely to be independent of the BTR complex. The helicase activity of BLM appears to

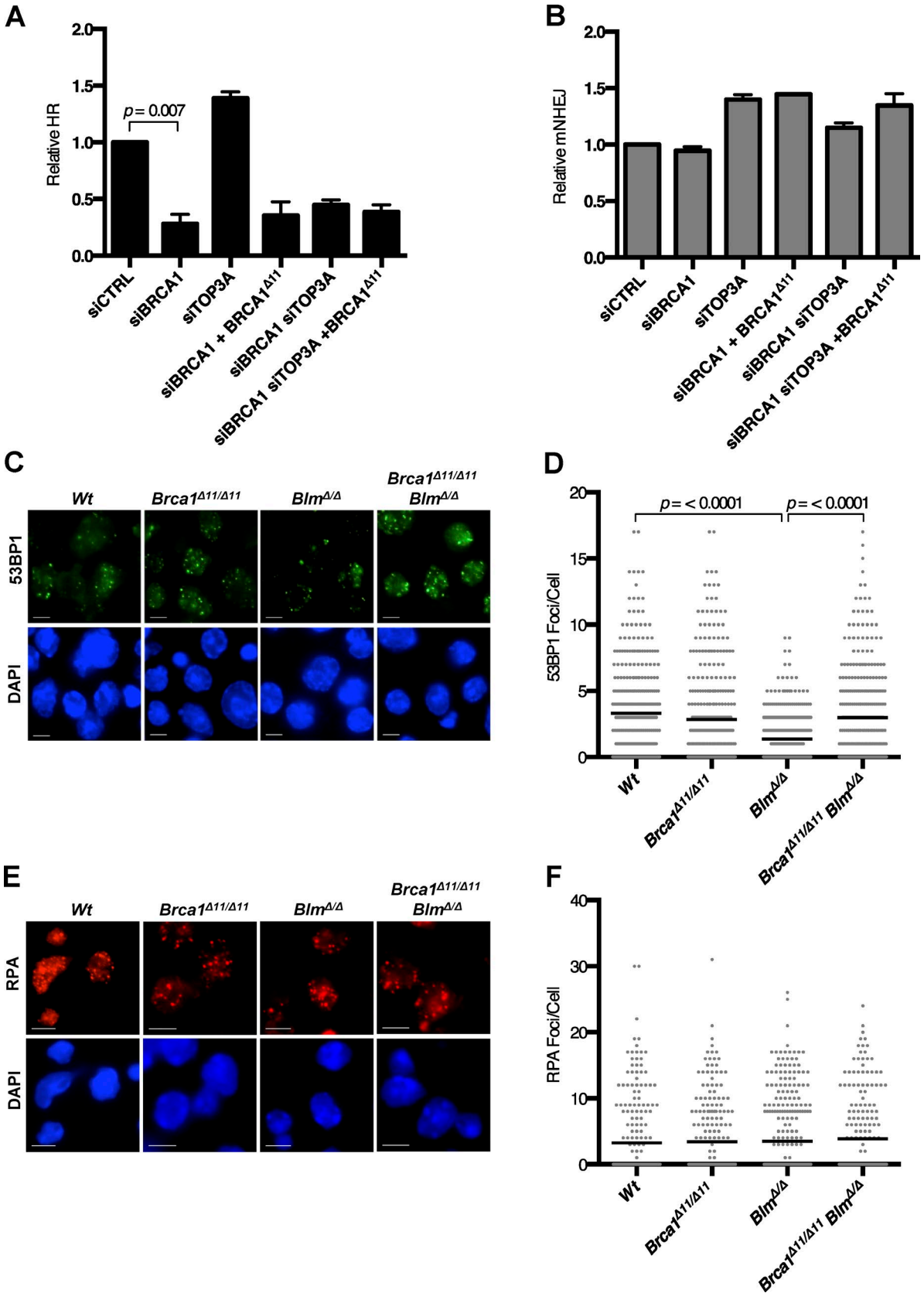

Figure 5. **Ablation of *Blm* increases 53BP1 accumulation at DNA break sites in *Brca1*$^{\Delta 11/\Delta 11}$ cells.** (A) Analysis of relative HR frequency in the EJ-DR U2OS reporter cell line after knockdown of *BRCA1* and *TOP3A* and overexpression of BRCA1$^{\Delta 11}$. (B) Analysis of relative mutagenic NHEJ (mNHEJ) frequency in the EJ-DR U2OS reporter cell line. (C) Immunofluorescence analysis of 53BP1 IRIF in primary B cells from mice of indicated genotypes after IR. (D) Quantification of 53BP1 IRIF in primary B cells. (E) Immunofluorescence analysis of RPA IRIF in primary B cells from indicated genotypes after IR. (F) Quantification of RPA IRIF in primary B cells. Graphs represent mean ± SD of three independent experiments. Bars, 10 µm.

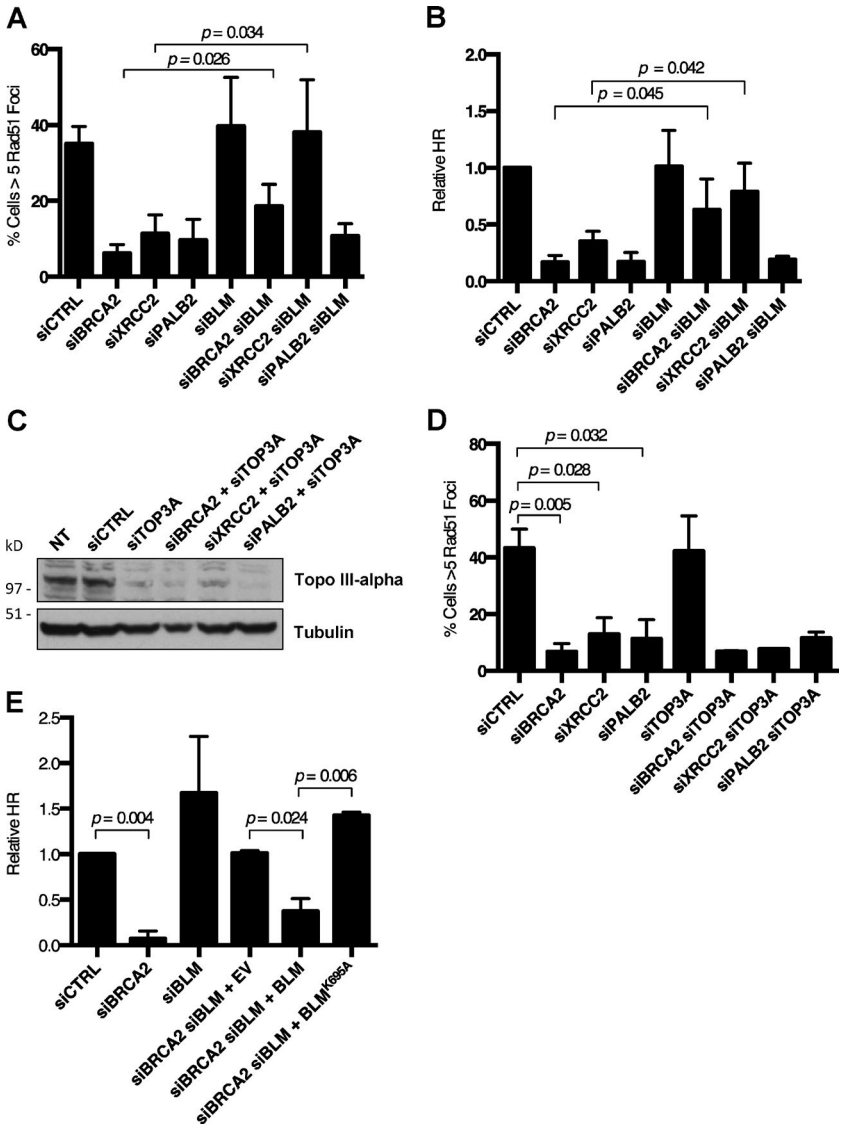

Figure 6. **Rescue of RAD51 IRIF and HR in BRCA2- and XRCC2-deficient cells by silencing of *BLM* requires BLM helicase activity, but not TOP3A.** (A) Quantification of RAD51 IRIF in U2OS cells after indicated knockdowns and IR. (B) Analysis of relative HR frequency in the U2OS EJ-DR reporter cell line after indicated knockdown. (C) Western blot analysis of *TOP3A* knockdown efficiency in U2OS cells with no treatment (NT) and indicated siRNA-mediated knockdowns. (D) Quantification of RAD51 IRIF in U2OS cells after indicated knockdowns and IR. (E) Analysis of relative HR frequency in the U2OS EJ-DR reporter cell line after indicated knockdowns. Graphs represent mean ± SD of three independent experiments.

influence HR in siBRCA2 cells, however. Expression of exogenous BLM^{WT} in siBRCA2 cells reversed the rescue of HR that was achieved by knockdown of *BLM*, but an equivalent effect was not observed upon expression of the helicase-dead BLM^{K695A} mutant (Fig. 6 E). Collectively with our other data (Fig. 4 F), this result suggests that the helicase activity of BLM is essential for its anti-recombinase effect in cells of several different genetic backgrounds.

Several enzymes have been reported to exhibit anti-recombinase activity in mammalian cells (Karpenshif and Bernstein, 2012). We performed siRNA knockdown of three of these factors to evaluate if they could rescue HR in cells lacking BRCA2 or XRCC2 (Fig. S5, A–C). First, we tested the RECQ5/*RECQL5* helicase, which is reported to have anti-recombinase activity (Hu et al., 2007). Although *BLM* knockdown can partially rescue the defect in RAD51 foci and HR in cells treated with siBRCA2 or siXRCC2 (Fig. 6, A and B), equivalent knockdown of *RECQL5* had little effect (Fig. 7, A and B). FBH1 is a second protein that has been reported to act as a mammalian anti-recombinase, and WRN is a RECQ helicase that has been shown to target RAD51-loaded DNA structures (Constantinou et al., 2000; Fugger et al., 2009; Wang et al., 2015). To evaluate the effect of these factors on recombination efficiency, we repeated our HR assay in siBRCA2 and siXRCC2 cells with combined knockdown of either *FBH1* or *WRN* (Fig. 7 C). Knockdown of *WRN* or *FBH1* afforded a rescue of HR in siXRCC2 cells. Knockdown of *WRN* also gave a partial rescue of HR in siBRCA2 cells, but no significant difference in HR efficiency was observed in these cells upon knockdown of *FBH1*. The efficiency of NHEJ was not affected in any case (Fig. 7 D). We conclude that the ability of BLM to suppress HR is of an equivalent magnitude to that seen with other mammalian anti-recombinases, at least in cells that are HR deficient.

Discussion

Regulation of HR through altered stability of the RAD51 nucleoprotein filament

Our results show that BLM promotes genomic instability in HR-deficient cells, to a level that can cause cell death, by reducing the stability of RAD51 at the presynaptic filament. BLM appears to act by disrupting RAD51 on resected DNA ends. In

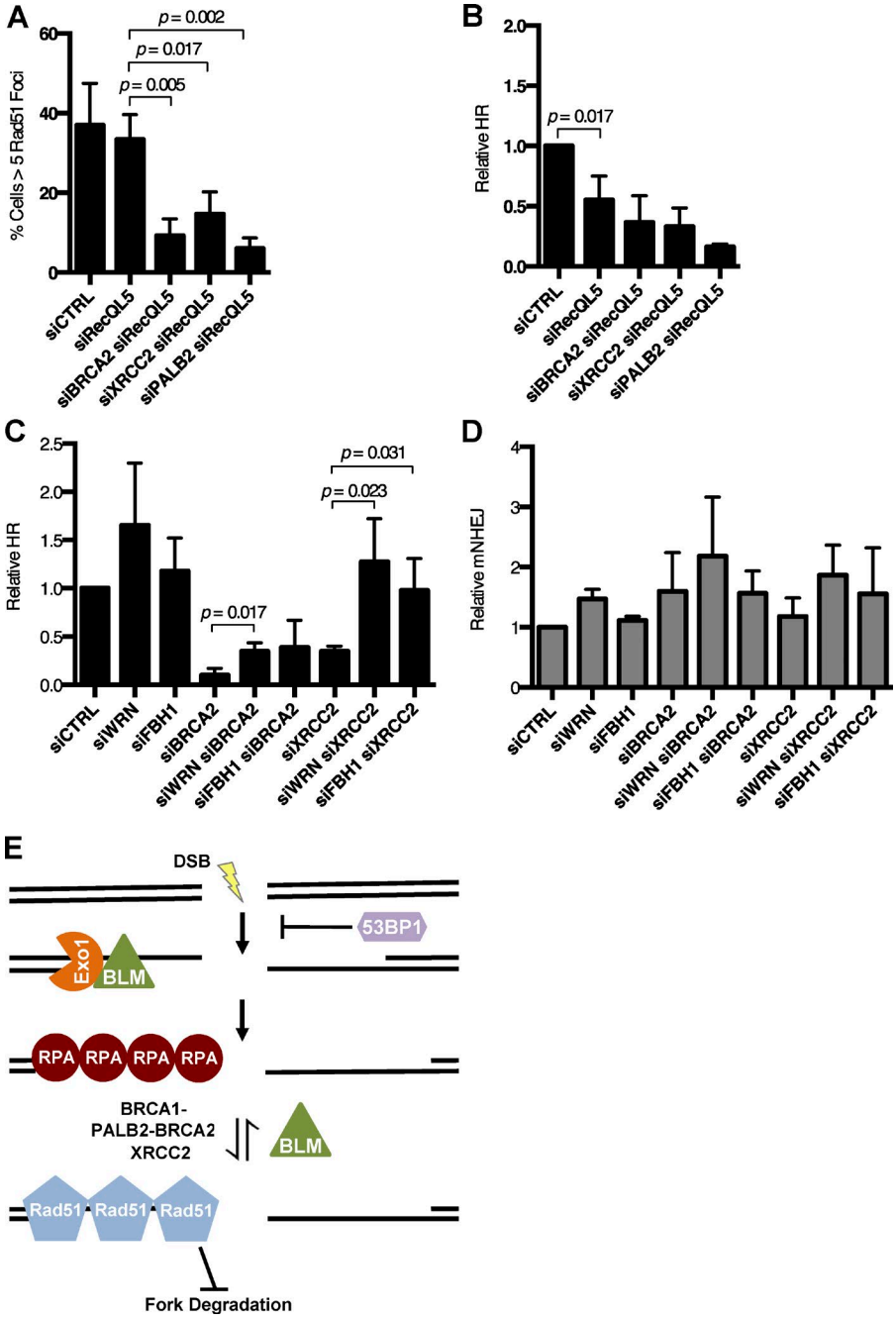

Figure 7. **Effect of pro- and anti-recombinogenic proteins on HR efficiency.** (A) Quantification of RAD51 IRIF in U2OS cells after indicated knockdowns and IR. (B and C) Analysis of relative HR frequency in the EJ-DR U2OS reporter cell line after indicated knockdowns and *I-Sce1* induction. (D) Analysis of relative mutagenic NHEJ (mNHEJ) frequency in the EJ-DR U2OS reporter cell line after indicated knockdowns and *I-Sce1* induction. (E) Model for BLM acting as an anti-recombinogenic factor at the level of RAD51 loading to regulate efficient HR. Graphs represent mean ± SD of three independent experiments.

WT cells, the presence of BRCA1, BRCA2, and factors including XRCC2 stabilizes the RAD51 nucleoprotein filament despite the anti-recombinogenic effect of BLM, but when these factors are absent, there is a failure to retain RAD51 at the break site that leads to insufficient HR, genomic instability, and loss of cell viability (Fig. 7 E). Hyperaccumulation of RAD51 at DNA damage sites in BS cells has been observed previously (Bischof et al., 2001; Wu et al., 2001), and an ability of BLM to displace RAD51 from single-stranded DNA is supported by several lines of cellular and biochemical evidence (Bugreev et al., 2007; Tripathi et al., 2007, 2008). This work is the first to demonstrate that this activity has substantial physiological importance. This ability of BLM is distinct from proposed roles for the protein in DSB resection (Gravel et al., 2008; Nimonkar et al., 2008, 2011), D-loop displacement (van Brabant et al., 2000; Bachrati et al., 2006), or Holliday junction dissolution (Wu and Hickson, 2003).

Several cellular factors have been shown to maintain replication fork integrity by stabilizing RAD51 filaments (Schlacher et al., 2012; Leuzzi et al., 2016; Sato et al., 2016), and we find an equivalent role for BLM. Deletion of *Blm* largely rescues the fork degradation that is normally seen in *Brca1*$^{\Delta 11/\Delta 11}$ cells (Fig. 2, F and G), suggesting that BLM influences both HR efficiency and fork protection by regulating RAD51 filament stability. Interestingly, silencing of *BLM* has been reported to help protect replication forks and maintain genomic integrity in cells lacking the replication-associated protein BOD1L (Higgs et al., 2015). Targeting the anti-recombinase activity of BLM may therefore rescue genomic integrity in an even greater range of genotypes than those that we have tested in this study.

BLM as an Srs2-like anti-recombinase

Like BLM, the DNA damage response factor 53BP1 also regulates the efficiency of HR, albeit by a different mechanism (Bouwman et al., 2010; Bunting et al., 2010). 53BP1 limits DSB resection, thereby inhibiting HR and promoting use of alternative pathways for DSB repair such as NHEJ. The effect of BLM appears to be exerted at the level of stabilization of RAD51 on the resected 3′ single-stranded DNA region. This direct effect on RAD51 is reminiscent of the anti-recombinogenic effect of Srs2 during HR in *Saccharomyces cerevisiae.* Diploid yeast lacking Srs2 are hyperrecombinogenic and exhibit hypersensitivity to UV and IR, which can be rescued by mutations in RAD51 (Aboussekhra et al., 1989, 1992). Srs2 stimulates the ATPase activity of RAD51 at resected DSBs, promoting release of RAD51, and limiting the formation of an active presynaptic filament (Krejci et al., 2003; Veaute et al., 2003). Previous biochemical work has shown that the K695A mutant of BLM, which lacks DNA translocase and helicase activity, is not able to displace RAD51 from DNA templates in vitro (Bugreev et al., 2007). Our cell biological assays support the idea that the helicase activity of BLM is critical for its anti-recombinase function. Our work additionally shows that the association of BLM with topoisomerase IIIα, RMI-1, and RMI-2 as the BTR complex, which is essential for Holliday junction dissolution, is likely dispensable for its anti-recombinase activity.

BLM is one of a group of mammalian anti-recombinases

Although no precise mammalian orthologue of Srs2 has been identified, several proteins have been suggested to have an analogous function. These include FBH1, RECQ5, PARI, and POLQ (Hu et al., 2007; Fugger et al., 2009; Schwendener et al., 2010; Moldovan et al., 2012; Simandlova et al., 2013; Ceccaldi et al., 2015). It is not clear which of these proteins is of greatest importance for regulation of mammalian HR (Kowalczykowski, 2015). In our work, we measured the effect of ablation of BLM and the putative anti-recombinases, RECQ5, WRN, and FBH1 on the efficiency of HR in cells lacking key HR factors. We found that depletion of BLM has at least as significant an effect as depletion of these other putative anti-recombinases (Fig. 7, A–C). These results raise an important question of whether these factors act redundantly or are regulated to work in specific instances. Notably, BLM and RECQ5 act in a nonredundant fashion to suppress crossover recombination (Wang et al., 2003; Hu et al., 2005).

Effect of BLM on HR in BRCA2-, XRCC2-, and PALB2-deficient cells

Whereas our overexpression analysis suggests that BLM works as an active anti-recombinase in normal cells, the effects of the absence of the anti-recombinase activity of BLM was most easily observed in cells with deficiencies in HR. In addition to its effect in *Brca1*$^{\Delta 11/\Delta 11}$ cells, deletion of *BLM* afforded some degree of rescue of the HR defect normally seen in siBRCA2 and siXRCC2 cells. Deletion of *BLM* did not, however, afford any substantial rescue of HR in PALB2-deficient cells. This result was unexpected, because PALB2 interacts with both BRCA1 and BRCA2 to allow stable association of BRCA2 at DSB sites and loading of RAD51 (Xia et al., 2006; Sy et al., 2009b; Zhang et al., 2009). As PALB2 deficiency is not rescued by *BLM* deletion, it is possible that PALB2 plays a role separate from BRCA1 and BRCA2 in the control of genomic integrity or RAD51 loading. Notably, PALB2 has been shown to directly interact with D-loop structures, where it is able to interact with and stabilize RAD51 (Buisson et al., 2010). PALB2 also binds MRG15, a chromodomain protein that modifies the efficiency of HR (Sy et al., 2009a). Clearly, the full range of activities that regulate the stability of the RAD51 nucleoprotein filament warrants further study.

Our results support a hypothesis in which a failure to constrain mutagenic RAD51-dependent processes such as nonallelic HR may lead to the chromosome instability seen in BS cells (Bhargava et al., 2016; Carvalho and Lupski, 2016). *SGS1*, the yeast homologue of *BLM*, suppresses recombination between homologous sequences and can partially substitute for Srs2 in *srs2* mutant yeast (Myung et al., 2001; Mankouri et al., 2002; Ira et al., 2003). Deletion of *Blm* in mouse spermatocytes also leads to a block in meiosis associated with mispairing of homologous chromosomes and increased chiasmata (Holloway et al., 2010). We propose that BLM deserves further consideration as an anti-recombinase with substantial importance in regulating the HR pathway for repair of mammalian DSBs.

Materials and methods

Cell culture

Resting primary B cells were isolated from mouse spleen by ACK lysis of erythrocytes and negative selection with anti-CD43 MACS microbeads (Miltenyi). B cells were resuspended at 0.5–1 × 10^6 cells/ml and activated with 25 µg/ml lipopolysaccharide (L2630; Sigma Aldrich), 50 U/ml IL-4 (I1020; Sigma Aldrich), and 1:1,000 RP105 antibody (55128; BD) for 48–72 h. MEFs as well as U2OS, MDA-MB-231, and MDA-MB-436 cells were cultured in DMEM supplemented with 15% FBS and 1% penicillin/streptomycin.

DNA repair assay

The EJ-DR assay was performed as previously described (Bindra et al., 2013). EJ-DR reporter cells were plated at 200,000–500,000 cells per well in 10% charcoal-stripped FBS (100–119; Gemini), antibiotic/antimycotic, and DMEM and transfected the next day with siRNA and/or plasmid DNA using Lipofectamine 2000 (11668; Invitrogen) or Lipofectamine RNAiMAX (13778; Invitrogen). After knockdown and expression (24 h), cells were grown in 10% Tet-free FBS (100-800; Gemini), antibiotic/antimycotic, and DMEM. Incorporated *I-Sce1* was induced with Shield1 (632189; Clontech) and triamcinolone (T6510; Sigma Aldrich) ligands for 24 h. NHEJ and HR repair activity was assessed 48 h postinduction by quantification of DsRed- and GFP-positive cells on BD FACS Calibur system and analyzed on FlowJo (Tree Star).

Metaphase spreads

Telomere DNA FISH analysis was performed and analyzed as previously described (Misenko and Bunting, 2014). B cells were activated for 24 h and treated with 250 nM mitomycin C (Sigma Aldrich), 2 µM olaparib (KU0059436; Selleckchem), or 4 µM cisplatin (Sigma Aldrich) for 16 h. Cells were arrested in metaphase with 100 ng/ml colcemid (Sigma Aldrich) for 1 h. Cells were collected, incubated in hypotonic solution (0.075 M KCl) for 15 min at 37°C, and fixed in a 3:1 methanol/acetic acid solution (three washes) and stored overnight at −20°C. Cells were dropped onto glass microscope slides in a Thermotron at 52% humidity at 22.9°C and dried for 30 min to 1 h and stored in 37°C chamber. Telomere DNA FISH analysis was performed by first preparing the telomeric Cy-3 PNA probe (Cy3-00-CCCTAA CCCTAACCCTAA, F1002; PNA Bio Inc.). The probe was incubated

in deionized formamide, pH 7.0, at 37°C for 1 h, followed by addition of FISH Master Mix (4× SSC, 20% dextran sulfate) and incubation in at 37°C for 1 h. Probe was denatured at 80°C followed by preannealing at 37°C for 1 h.

Concurrently, chromosome slides were pretreated with pepsin in 0.01 M HCl acidic solution for 90 s at 37°C, followed by washes in 1× PBS and 1× PBS/50 mM $MgCl_2$, and fixed in 1% formaldehyde/1× PBS/50 mM $MgCl_2$ for 10 min. Slides were then washed in 1× PBS, dehydrated in a series of ethanol incubations (70%, 90%, and 100%), and air dried. Slides were denatured by incubation at 80°C in 70% deionized formamide/2× SSC for 90 s, followed by dehydration in a series of ethanol incubations (70%, 90%, and 100%), and air dried. In a humidity chamber, the preannealed probe mix was applied to the slide, covered with 18 × 18 mm coverslip, and incubated for 1 h at 37°C. The probe was cross-linked in 50% formamide/2× SSC (three 5-min washes), followed by washes in 1× SSC (3 × 5 min washes) and 1× SSC/0.1% Tween 20 (three 5-min washes). Slides were counterstained in DAPI solution, washed in 3× SSC, and mounted in Mowiol antifade solution. For each experiment, 50 metaphases per genotype and treatment were analyzed.

Animal husbandry

All animal experiments were approved by the Institutional Animal Care and Use Committee at Rutgers University (protocol 12–024).

Flow cytometry

Primary T cells were isolated from thymi of 2- to 3-mo-old mice in 1× HBSS, 1% FBS/1× penicillin/streptomycin and strained through a 70-µm mesh. Blocking was with anti–CD16/CD32 antibody (rat, 553142; BD Biosciences) and stained with APC-CD8a (rat; 553035; BD Biosciences) and/or FITC-CD4 (rat, 553046; BD Biosciences) antibodies. For analysis of CSR, B cells were stained with 1:100 dilutions of anti-B220-FITC (rat; 553088, BD Biosciences) and biotin anti–mouse IgG1 (rat, 553441; BD) followed by incubation in streptavidin Alexa Fluor 647 (S32357; Thermo Fisher). Cells were washed twice in 1× HBSS, 1% FBS, and 1× penicillin/streptomycin. For analysis of RPA staining, B cells treated with 10 Gy IR followed by 2 h of recovery were extracted with PBS with Tween 20, fixed in 4% PFA, permeabilized, and stained with RPA32 antibody (rat, 1:500, 2208; Cell Signaling). After secondary staining with Alexa Flour 488 anti-rat (1:200; A11006; Life Technologies), cells were stained for DNA content using propidium iodide (Forment et al., 2012). Flow cytometry analysis was performed on BD FACSCalibur system and analyzed on FlowJo (Tree Star).

Sister chromatid exchange assay

B cells were activated in the presence of 10 µm BrdU for 48 h followed by arrest in metaphase with 100 ng/ml colcemid (Sigma Aldrich). Cells were fixed and dropped onto glass slides for metaphase spreads (see Materials and Methods). Slides were stained with Hoechst 33258 (Thermo Fisher), incubated in McIlvaine's solution (164 mM Na_2HPO_4, 16 mM citric acid, pH 7.0), and exposed to UV light for 45 min. Slides were incubated in a 1:12 Giemsa staining solution in 3% methanol, dehydrated with xylenes, and mounted with Permount (Fisher Scientific).

DNA combing

Splenic B cells were grown in vitro for 48 h under activating conditions. Cells were incubated with 25 µM 5-iododeoxyuridine (I7125; Sigma Aldrich) for 20 min followed by a 20 min incubation with 250 µM 5-chlorodeoxyuridine (C6891; Sigma Aldrich). Cells were subsequently treated with 4mM hydroxyurea for five hours (H8627; Sigma Aldrich). DNA fiber spreads were prepared and analyzed by immunofluorescence as previously described (Li et al., 2016). Cell suspension was collected in 2-µl volume and dried on glass slide. Cells were lysed in 7 µl lysis buffer consisting of 50 mM EDTA and 0.5% SDS in 200 mM Tris-HCl, pH 7.5, for 2 min. Slides were tilted at 15° angle to dry and create spread of DNA fibers. Slides were fixed in methanol/acetic acid solution (3:1) for 10 min followed by incubation in 2.5M HCl for 80 min. Slides were washed with PBS, blocked in 5% BSA for 20 min, and stained with 1:25 anti-BrdU (mouse) and 1:400 anti-BrdU (rat) in 5% BSA for 2 h in a humidity chamber. Slides were washed with PBS and stained with 1:500 sheep anti–mouse Cy3 and 1:400 goat anti–rat Alexa Fluor 488 secondary antibody for 1 h. Slides were again washed in PBS and mounted using Vectashield mounting medium with glass coverslips. Approximately 300 fiber lengths were analyzed per genotype in three independent experiments using ImageJ software.

Western blotting and immunofluorescence

Primary antibodies were used at the following dilutions for Western blotting: anti-tubulin (mouse, 1:50,000; Sigma Aldrich), mouse anti-BLM (rabbit, 1:1,000; A300-110A; Bethyl), human anti-BLM (rabbit, 1:1,000; ab2179; Abcam), anti-BRCA1 (mouse, 1:1,000; MABC199; EMD Millipore), anti-RECQ5 (rabbit, 1:1,000; ab31609; Abcam), anti-TOP3A (rabbit, 1:2,000; 14525-1-AP; Proteintech), anti-XRCC2 (mouse, 1:1,000; ab20253; Abcam), anti-BRCA2 (rabbit, 1:1,000; sc28235; Santa Cruz), anti-WRN (mouse, 1:500; ab66606; Abcam), anti-FBH1 (mouse, 1:1,000; sc-81563; Santa Cruz), and anti-PALB2 (1:1,000, M11, raised in rabbits against amino acids 601–880 of human PALB2). Secondary HRP-conjugated anti–mouse (sheep; 1:2,000; NA931V; GE Healthcare) and anti–mouse (donkey; 1:2,000; NA9340V; GE Healthcare) antibodies were used.

For immunofluorescence, U2OS, MEF, and MDA-231/436 cells were grown on 18 × 18-mm coverslips overnight before 10 Gy IR treatment and 2-h recovery. B lymphocyte cells were activated and treated with 10 Gy IR and 4 h recovery before being dropped onto slides coated with Cell-tak (BD). Cells were preextracted in 0.5% Triton X-100 in PBS, fixed in 2% paraformaldehyde in PBS, and permeabilized in 0.5% Triton X-100 in PBS and incubated in antibody. Primary antibodies were used at the following dilutions: anti-RAD51 (rabbit, 1:100; H-92; Santa Cruz), anti-53BP1 (rabbit, 1:2,000; NB100-304; Novus), and anti-RPA32 (rat, 1:100; 2208; Cell Signaling) and detected with anti–rabbit Alexa Fluor 546 or Alexa Fluor 488 antibody (1:200; Thermo Fisher) or anti–rat Alexa Fluor 488 (1:200; Life Technologies). Cells were counterstained with DAPI and mounted in Mowiol solution. Approximately 200–500 cells per treatment were analyzed for each experiment.

Plasmids

The BRCA1 expression constructs were based on pcDNA-3xMyc-BRCA1, which was provided by B. Xia (Rutgers Cancer Institute of New Jersey, New Brunswick, NJ) and has been previously described (Chen et al., 1998; Anantha et al., 2017). The $BRCA1^{\Delta 11}$ construct was generated through site-directed mutagenesis following the QuikChange protocol (Agilent Technologies).

The full-length *hBLM* was PCR amplified from the pGFP-C1-BLM (80070; Addgene), provided by N. Ellis (The University of Arizona Cancer Center, Tuscon, AZ; Hu et al., 2001), using the iPROOF High-Fidelity PCR kit (Bio-Rad) and a 3′ primer (5′-TGCT TTAATT AATTACTTGTCGTCATCGTCCTTGTAGTCTGAGAATGCATATG AAGGCTTAAGAAACGGTCTATT-3′) containing codons for the FLAG epitope tag (DYKDDDDK). The amplified product was ligated into the pMx-GFP vector by restriction digest with Xho1 and Pac1 to generate the pMx-GFP-hBLMFLAG construct. The BLM^{K695A} construct was generated through site-directed mutagenesis following the QuikChange protocol (Agilent Technologies).

siRNA and shRNA

For depletion of *BLM* by shRNA, a pLKO.1 plasmid containing the targeting sequence (5′-CCGGCGAAGGAAACTCACGTCAATACTCGAGTATTGACGTGAGTTTCCTTCGTTTTTG-3′; TRCN-0000070996; Sigma Aldrich) for MEFs, a pLKO.1 plasmid containing the targeting sequence (5′-GCCTTTATTCAATACCCATTT-3′; TRCN0000004904; Sigma Aldrich) for human cells, or control vector was transfected into 293T cells with pMD2.G and pVSVG plasmids to produce lentivirus. MEF cells were infected with lentivirus and selected in medium containing 2 µg/ml puromycin for 1 wk and maintained in 1 µg/ml puromycin thereafter. For transient knockdown via siRNA, siGENOME SMARTpool constructs targeting BLM, BRCA2, XRCC2, PALB2, TOP3A, RecQ5, FBH1, and WRN were acquired commercially (Dharmacon; Table S1) and transfected into U2OS and U2OS EJ-DR reporter cell lines. Custom siRNAs targeting the 3′-UTR region of *BRCA1* and *BLM* were used for knockdown and mutant expression experiments (Table S2). Knockdown efficiency was confirmed via Western blot analysis.

Microscopy

Metaphase spreads were mounted in Mowiol solution and imaged at room temperature using an AxioImager.Z2 microscope (Zeiss) with a Plan-Apo 60×/1.4 oil objective lens (Nikon). The microscope was fitted with a CoolCube 1m camera system and MetaSystems Metafer automatic slide platform. Acquisition of images was performed using Metafer4 v3.9.6 software and images were viewed in Photoshop CS6 (Adobe). Immunofluorescence slides were mounted in Mowiol solution and imaged at room temperature using an E800 microscope (Nikon) with anApochromat 63×/1.4 oil objective lens (Zeiss). The microscope was fitted with a DXM1200F camera system (Nikon). Acquisition of images was performed using ACT-1 software (Nikon) and viewed and overlaid in PhotoShop CS6.

Statistical analysis

All experiments were performed with a minimum of three independent experiments. Data and statistical analysis was performed on GraphPad Prism 6. Error bars represent standard deviation between experiments. P-values were calculated using a Student's *t* test.

Online supplemental material

Fig. S1 shows that ablation of *Blm* rescues genomic instability in *Brca1*$^{\Delta 11/\Delta 11}$ cells. Fig. S2 shows an analysis of SCEs in *Brca1*$^{\Delta 11/\Delta 11}$;*Blm*$^{\Delta/\Delta}$ cells and BLM overexpression and Rad51 foci in U2OS cells. Fig. S3 shows that ablation of *Blm* increases CSR in *Brca1*$^{\Delta 11/\Delta 11}$ cells but has no effect on RPA intensity. Fig. S4 shows knockdown of *PALB2*, *BRCA2*, and *XRCC2* in U2OS cells. Fig. S5 shows knockdown of *RECQ5*, *FBH1*, and *WRN* anti-recombination factors in U2OS cells. Table S1 lists the Dharmacon siRNA oligonucleotides used. Table S2 lists the custom siRNA oligos used.

Acknowledgments

The authors thank Dr. Bing Xia for providing the pcDNA-3xMyc-BRCA1 plasmid and Dr. Steve Brill and Dr. Bing Xia for critical review of the manuscript.

This work was funded by National Institutes of Health grant R01CA190858 (to S.F. Bunting). D.S. Patel and S.M. Misenko are supported by New Jersey Commission on Cancer Research predoctoral fellowships and the National Institutes of Health Ruth L. Kirschstein National Research service award T32 GM8339.

The authors declare no competing financial interests.

Author contributions: D.S. Patel and S.F. Bunting designed experiments. D.S. Patel performed the experimental procedures. S.M. Misenko performed analysis of SCEs. J. Her performed the DNA fiber assay.

Submitted: 21 March 2017
Revised: 28 June 2017
Accepted: 4 August 2017

References

Aboussekhra, A., R. Chanet, Z. Zgaga, C. Cassier-Chauvat, M. Heude, and F. Fabre. 1989. RADH, a gene of *Saccharomyces cerevisiae* encoding a putative DNA helicase involved in DNA repair. Characteristics of radH mutants and sequence of the gene. *Nucleic Acids Res.* 17:7211–7219. http://dx.doi.org/10.1093/nar/17.18.7211

Aboussekhra, A., R. Chanet, A. Adjiri, and F. Fabre. 1992. Semidominant suppressors of Srs2 helicase mutations of *Saccharomyces cerevisiae* map in the RAD51 gene, whose sequence predicts a protein with similarities to procaryotic RecA proteins. *Mol. Cell. Biol.* 12:3224–3234. http://dx.doi.org/10.1128/MCB.12.7.3224

Anantha, R.W., S. Simhadri, T.K. Foo, S. Miao, J. Liu, Z. Shen, S. Ganesan, and B. Xia. 2017. Functional and mutational landscapes of BRCA1 for homology-directed repair and therapy resistance. *eLife.* 6: e21350. http://dx.doi.org/10.7554/eLife.21350

Bachrati, C.Z., R.H. Borts, and I.D. Hickson. 2006. Mobile D-loops are a preferred substrate for the Bloom's syndrome helicase. *Nucleic Acids Res.* 34:2269–2279. http://dx.doi.org/10.1093/nar/gkl258

Bhargava, R., D.O. Onyango, and J.M. Stark. 2016. Regulation of single-strand annealing and its role in genome maintenance. *Trends Genet.* 32:566–575. http://dx.doi.org/10.1016/j.tig.2016.06.007

Bhattacharyya, A., U.S. Ear, B.H. Koller, R.R. Weichselbaum, and D.K. Bishop. 2000. The breast cancer susceptibility gene BRCA1 is required for subnuclear assembly of Rad51 and survival following treatment with the DNA cross-linking agent cisplatin. *J. Biol. Chem.* 275:23899–23903. http://dx.doi.org/10.1074/jbc.C000276200

Bindra, R.S., A.G. Goglia, M. Jasin, and S.N. Powell. 2013. Development of an assay to measure mutagenic non-homologous end-joining repair activity in mammalian cells. *Nucleic Acids Res.* 41:e115. http://dx.doi.org/10.1093/nar/gkt255

Bischof, O., S.H. Kim, J. Irving, S. Beresten, N.A. Ellis, and J. Campisi. 2001. Regulation and localization of the Bloom syndrome protein in response to DNA damage. *J. Cell Biol.* 153:367–380. http://dx.doi.org/10.1083/jcb.153.2.367

Bouwman, P., A. Aly, J.M. Escandell, M. Pieterse, J. Bartkova, H. van der Gulden, S. Hiddingh, M. Thanasoula, A. Kulkarni, Q. Yang, et al. 2010. 53BP1 loss rescues BRCA1 deficiency and is associated with triple-negative and BRCA-mutated breast cancers. *Nat. Struct. Mol. Biol.* 17:688–695. http://dx.doi.org/10.1038/nsmb.1831

Bugreev, D.V., X. Yu, E.H. Egelman, and A.V. Mazin. 2007. Novel pro- and anti-recombination activities of the Bloom's syndrome helicase. *Genes Dev.* 21:3085–3094. http://dx.doi.org/10.1101/gad.1609007

Buisson, R., A.M. Dion-Côté, Y. Coulombe, H. Launay, H. Cai, A.Z. Stasiak, A. Stasiak, B. Xia, and J.Y. Masson. 2010. Cooperation of breast cancer proteins PALB2 and piccolo BRCA2 in stimulating homologous recombination. *Nat. Struct. Mol. Biol.* 17:1247–1254. http://dx.doi.org/10.1038/nsmb.1915

Bunting, S.F., E. Callén, N. Wong, H.T. Chen, F. Polato, A. Gunn, A. Bothmer, N. Feldhahn, O. Fernandez-Capetillo, L. Cao, et al. 2010. 53BP1 inhibits homologous recombination in Brca1-deficient cells by blocking resection of DNA breaks. *Cell.* 141:243–254. http://dx.doi.org/10.1016/j.cell.2010.03.012

Carvalho, C.M., and J.R. Lupski. 2016. Mechanisms underlying structural variant formation in genomic disorders. *Nat. Rev. Genet.* 17:224–238. http://dx.doi.org/10.1038/nrg.2015.25

Ceccaldi, R., J.C. Liu, R. Amunugama, I. Hajdu, B. Primack, M.I. Petalcorin, K.W. O'Connor, P.A. Konstantinopoulos, S.J. Elledge, S.J. Boulton, et al. 2015. Homologous-recombination-deficient tumours are dependent on Polθ-mediated repair. *Nature.* 518:258–262. http://dx.doi.org/10.1038/nature14184

Chaganti, R.S., S. Schonberg, and J. German. 1974. A manyfold increase in sister chromatid exchanges in Bloom's syndrome lymphocytes. *Proc. Natl. Acad. Sci. USA.* 71:4508–4512. http://dx.doi.org/10.1073/pnas.71.11.4508

Chapman, J.R., M.R. Taylor, and S.J. Boulton. 2012. Playing the end game: DNA double-strand break repair pathway choice. *Mol. Cell.* 47:497–510. http://dx.doi.org/10.1016/j.molcel.2012.07.029

Chen, J., D.P. Silver, D. Walpita, S.B. Cantor, A.F. Gazdar, G. Tomlinson, F.J. Couch, B.L. Weber, T. Ashley, D.M. Livingston, and R. Scully. 1998. Stable interaction between the products of the BRCA1 and BRCA2 tumor suppressor genes in mitotic and meiotic cells. *Mol. Cell.* 2:317–328. http://dx.doi.org/10.1016/S1097-2765(00)80276-2

Chester, N., H. Babbe, J. Pinkas, C. Manning, and P. Leder. 2006. Mutation of the murine Bloom's syndrome gene produces global genome destabilization. *Mol. Cell. Biol.* 26:6713–6726. http://dx.doi.org/10.1128/MCB.00296-06

Chu, W.K., K. Hanada, R. Kanaar, and I.D. Hickson. 2010. BLM has early and late functions in homologous recombination repair in mouse embryonic stem cells. *Oncogene.* 29:4705–4714. http://dx.doi.org/10.1038/onc.2010.214

Constantinou, A., M. Tarsounas, J.K. Karow, R.M. Brosh, V.A. Bohr, I.D. Hickson, and S.C. West. 2000. Werner's syndrome protein (WRN) migrates Holliday junctions and co-localizes with RPA upon replication arrest. *EMBO Rep.* 1:80–84. http://dx.doi.org/10.1093/embo-reports/kvd004

Ellis, N.A., J. Groden, T.Z. Ye, J. Straughen, D.J. Lennon, S. Ciocci, M. Proytcheva, and J. German. 1995. The Bloom's syndrome gene product is homologous to RecQ helicases. *Cell.* 83:655–666. http://dx.doi.org/10.1016/0092-8674(95)90105-1

Elstrodt, F., A. Hollestelle, J.H. Nagel, M. Gorin, M. Wasielewski, A. van den Ouweland, S.D. Merajver, S.P. Ethier, and M. Schutte. 2006. BRCA1 mutation analysis of 41 human breast cancer cell lines reveals three new deleterious mutants. *Cancer Res.* 66:41–45. http://dx.doi.org/10.1158/0008-5472.CAN-05-2853

Evers, B., and J. Jonkers. 2006. Mouse models of BRCA1 and BRCA2 deficiency: Past lessons, current understanding and future prospects. *Oncogene.* 25:5885–5897. http://dx.doi.org/10.1038/sj.onc.1209871

Forment, J.V., R.V. Walker, and S.P. Jackson. 2012. A high-throughput, flow cytometry-based method to quantify DNA-end resection in mammalian cells. *Cytometry A.* 81:922–928. http://dx.doi.org/10.1002/cyto.a.22155

Fugger, K., M. Mistrik, J.R. Danielsen, C. Dinant, J. Falck, J. Bartek, J. Lukas, and N. Mailand. 2009. Human Fbh1 helicase contributes to genome maintenance via pro- and anti-recombinase activities. *J. Cell Biol.* 186:655–663. http://dx.doi.org/10.1083/jcb.200812138

Grabarz, A., J. Guirouilh-Barbat, A. Barascu, G. Pennarun, D. Genet, E. Rass, S.M. Germann, P. Bertrand, I.D. Hickson, and B.S. Lopez. 2013. A role for BLM in double-strand break repair pathway choice: Prevention of CtIP/Mre11-mediated alternative nonhomologous end-joining. *Cell Reports.* 5:21–28. http://dx.doi.org/10.1016/j.celrep.2013.08.034

Gravel, S., J.R. Chapman, C. Magill, and S.P. Jackson. 2008. DNA helicases Sgs1 and BLM promote DNA double-strand break resection. *Genes Dev.* 22:2767–2772. http://dx.doi.org/10.1101/gad.503108

Hakim, O., W. Resch, A. Yamane, I. Klein, K.R. Kieffer-Kwon, M. Jankovic, T. Oliveira, A. Bothmer, T.C. Voss, C. Ansarah-Sobrinho, et al. 2012. DNA damage defines sites of recurrent chromosomal translocations in B lymphocytes. *Nature.* 484:69–74.

Hennet, T., F.K. Hagen, L.A. Tabak, and J.D. Marth. 1995. T-cell-specific deletion of a polypeptide N-acetylgalactosaminyl-transferase gene by site-directed recombination. *Proc. Natl. Acad. Sci. USA.* 92:12070–12074. http://dx.doi.org/10.1073/pnas.92.26.12070

Higgs, M.R., J.J. Reynolds, A. Winczura, A.N. Blackford, V. Borel, E.S. Miller, A. Zlatanou, J. Nieminuszczy, E.L. Ryan, N.J. Davies, et al. 2015. BOD1L is required to suppress deleterious resection of stressed replication forks. *Mol. Cell.* 59:462–477. http://dx.doi.org/10.1016/j.molcel.2015.06.007

Holloway, J.K., M.A. Morelli, P.L. Borst, and P.E. Cohen. 2010. Mammalian BLM helicase is critical for integrating multiple pathways of meiotic recombination. *J. Cell Biol.* 188:779–789. http://dx.doi.org/10.1083/jcb.200909048

Hu, P., S.F. Beresten, A.J. van Brabant, T.Z. Ye, P.P. Pandolfi, F.B. Johnson, L. Guarente, and N.A. Ellis. 2001. Evidence for BLM and Topoisomerase IIIalpha interaction in genomic stability. *Hum. Mol. Genet.* 10:1287–1298. http://dx.doi.org/10.1093/hmg/10.12.1287

Hu, Y., X. Lu, E. Barnes, M. Yan, H. Lou, and G. Luo. 2005. Recql5 and Blm RecQ DNA helicases have nonredundant roles in suppressing crossovers. *Mol. Cell. Biol.* 25:3431–3442. http://dx.doi.org/10.1128/MCB.25.9.3431-3442.2005

Hu, Y., S. Raynard, M.G. Sehorn, X. Lu, W. Bussen, L. Zheng, J.M. Stark, E.L. Barnes, P. Chi, P. Janscak, et al. 2007. RECQL5/Recql5 helicase regulates homologous recombination and suppresses tumor formation via disruption of Rad51 presynaptic filaments. *Genes Dev.* 21:3073–3084. http://dx.doi.org/10.1101/gad.1609107

Huber, L.J., T.W. Yang, C.J. Sarkisian, S.R. Master, C.X. Deng, and L.A. Chodosh. 2001. Impaired DNA damage response in cells expressing an exon 11-deleted murine Brca1 variant that localizes to nuclear foci. *Mol. Cell. Biol.* 21:4005–4015. http://dx.doi.org/10.1128/MCB.21.12.4005-4015.2001

Ira, G., A. Malkova, G. Liberi, M. Foiani, and J.E. Haber. 2003. Srs2 and Sgs1-Top3 suppress crossovers during double-strand break repair in yeast. *Cell.* 115:401–411. http://dx.doi.org/10.1016/S0092-8674(03)00886-9

Jensen, R.B., A. Carreira, and S.C. Kowalczykowski. 2010. Purified human BRCA2 stimulates RAD51-mediated recombination. *Nature.* 467:678–683. http://dx.doi.org/10.1038/nature09399

Johnson, R.D., N. Liu, and M. Jasin. 1999. Mammalian XRCC2 promotes the repair of DNA double-strand breaks by homologous recombination. *Nature.* 401:397–399. http://dx.doi.org/10.1038/43932

Karpenshif, Y., and K.A. Bernstein. 2012. From yeast to mammals: Recent advances in genetic control of homologous recombination. *DNA Repair (Amst.).* 11:781–788. http://dx.doi.org/10.1016/j.dnarep.2012.07.001

Kowalczykowski, S.C. 2015. An overview of the molecular mechanisms of recombinational DNA repair. *Cold Spring Harb. Perspect. Biol.* 7:a016410. http://dx.doi.org/10.1101/cshperspect.a016410

Krejci, L., S. Van Komen, Y. Li, J. Villemain, M.S. Reddy, H. Klein, T. Ellenberger, and P. Sung. 2003. DNA helicase Srs2 disrupts the Rad51 presynaptic filament. *Nature.* 423:305–309. http://dx.doi.org/10.1038/nature01577

Larsen, N.B., and I.D. Hickson. 2013. RecQ helicases: Conserved guardians of genomic integrity. *Adv. Exp. Med. Biol.* 767:161–184. http://dx.doi.org/10.1007/978-1-4614-5037-5_8

Leuzzi, G., V. Marabitti, P. Pichierri, and A. Franchitto. 2016. WRNIP1 protects stalled forks from degradation and promotes fork restart after replication stress. *EMBO J.* 35:1437–1451. http://dx.doi.org/10.15252/embj.201593265

Li, M., F. Cole, D.S. Patel, S.M. Misenko, J. Her, A. Malhowski, A. Alhamza, H. Zheng, R. Baer, T. Ludwig, et al. 2016. 53BP1 ablation rescues genomic instability in mice expressing 'RING-less' BRCA1. *EMBO Rep.* 17:1532–1541. http://dx.doi.org/10.15252/embr.201642497

Lorenz, A., F. Osman, V. Folkyte, S. Sofueva, and M.C. Whitby. 2009. Fbh1 limits Rad51-dependent recombination at blocked replication forks. *Mol. Cell. Biol.* 29:4742–4756. http://dx.doi.org/10.1128/MCB.00471-09

Luo, G., I.M. Santoro, L.D. McDaniel, I. Nishijima, M. Mills, H. Youssoufian, H. Vogel, R.A. Schultz, and A. Bradley. 2000. Cancer predisposition caused by elevated mitotic recombination in Bloom mice. *Nat. Genet.* 26:424–429. http://dx.doi.org/10.1038/82548

Mak, T.W., A. Hakem, J.P. McPherson, A. Shehabeldin, E. Zablocki, E. Migon, G.S. Duncan, D. Bouchard, A. Wakeham, A. Cheung, et al. 2000. Brca1 required for T cell lineage development but not TCR loci rearrangement. *Nat. Immunol.* 1:77–82. http://dx.doi.org/10.1038/76950

Manis, J.P., J.C. Morales, Z. Xia, J.L. Kutok, F.W. Alt, and P.B. Carpenter. 2004. 53BP1 links DNA damage-response pathways to immunoglobulin heavy chain class-switch recombination. *Nat. Immunol.* 5:481–487. http://dx.doi.org/10.1038/ni1067

Mankouri, H.W., T.J. Craig, and A. Morgan. 2002. SGS1 is a multicopy suppressor of srs2: Functional overlap between DNA helicases. *Nucleic Acids Res.* 30:1103–1113. http://dx.doi.org/10.1093/nar/30.5.1103

Manthei, K.A., and J.L. Keck. 2013. The BLM dissolvasome in DNA replication and repair. *Cell. Mol. Life Sci.* 70:4067–4084. http://dx.doi.org/10.1007/s00018-013-1325-1

Misenko, S.M., and S.F. Bunting. 2014. Rapid analysis of chromosome aberrations in mouse B lymphocytes by PNA-FISH. *J. Vis. Exp.* (90).

Moldovan, G.L., D. Dejsuphong, M.I. Petalcorin, K. Hofmann, S. Takeda, S.J. Boulton, and A.D. D'Andrea. 2012. Inhibition of homologous recombination by the PCNA-interacting protein PARI. *Mol. Cell.* 45:75–86. http://dx.doi.org/10.1016/j.molcel.2011.11.010

Moynahan, M.E., J.W. Chiu, B.H. Koller, and M. Jasin. 1999. Brca1 controls homology-directed DNA repair. *Mol. Cell.* 4:511–518. http://dx.doi.org/10.1016/S1097-2765(00)80202-6

Myung, K., A. Datta, C. Chen, and R.D. Kolodner. 2001. SGS1, the *Saccharomyces cerevisiae* homologue of BLM and WRN, suppresses genome instability and homeologous recombination. *Nat. Genet.* 27:113–116. http://dx.doi.org/10.1038/83673

Nimonkar, A.V., A.Z. Ozsoy, J. Genschel, P. Modrich, and S.C. Kowalczykowski. 2008. Human exonuclease 1 and BLM helicase interact to resect DNA and initiate DNA repair. *Proc. Natl. Acad. Sci. USA.* 105:16906–16911. http://dx.doi.org/10.1073/pnas.0809380105

Nimonkar, A.V., J. Genschel, E. Kinoshita, P. Polaczek, J.L. Campbell, C. Wyman, P. Modrich, and S.C. Kowalczykowski. 2011. BLM-DNA2-RPA-MRN and EXO1-BLM-RPA-MRN constitute two DNA end resection machineries for human DNA break repair. *Genes Dev.* 25:350–362. http://dx.doi.org/10.1101/gad.2003811

O'Regan, P., C. Wilson, S. Townsend, and J. Thacker. 2001. XRCC2 is a nuclear RAD51-like protein required for damage-dependent RAD51 focus formation without the need for ATP binding. *J. Biol. Chem.* 276:22148–22153. http://dx.doi.org/10.1074/jbc.M102396200

Ray Chaudhuri, A., E. Callen, X. Ding, E. Gogola, A.A. Duarte, J.E. Lee, N. Wong, V. Lafarga, J.A. Calvo, N.J. Panzarino, et al. 2016. Replication fork stability confers chemoresistance in BRCA-deficient cells. *Nature.* 535:382–387. http://dx.doi.org/10.1038/nature18325

Rickert, R.C., J. Roes, and K. Rajewsky. 1997. B lymphocyte-specific, Cre-mediated mutagenesis in mice. *Nucleic Acids Res.* 25:1317–1318. http://dx.doi.org/10.1093/nar/25.6.1317

Sato, K., M. Shimomuki, Y. Katsuki, D. Takahashi, W. Kobayashi, M. Ishiai, H. Miyoshi, M. Takata, and H. Kurumizaka. 2016. FANCI-FANCD2 stabilizes the RAD51-DNA complex by binding RAD51 and protects the 5′-DNA end. *Nucleic Acids Res.* 44:10758–10771. http://dx.doi.org/10.1093/nar/gkw876

Schlacher, K., H. Wu, and M. Jasin. 2012. A distinct replication fork protection pathway connects Fanconi anemia tumor suppressors to RAD51-BRCA1/2. *Cancer Cell.* 22:106–116. http://dx.doi.org/10.1016/j.ccr.2012.05.015

Schwendener, S., S. Raynard, S. Paliwal, A. Cheng, R. Kanagaraj, I. Shevelev, J.M. Stark, P. Sung, and P. Janscak. 2010. Physical interaction of RECQ5 helicase with RAD51 facilitates its anti-recombinase activity. *J. Biol. Chem.* 285:15739–15745. http://dx.doi.org/10.1074/jbc.M110.110478

Simandlova, J., J. Zagelbaum, M.J. Payne, W.K. Chu, I. Shevelev, K. Hanada, S. Chatterjee, D.A. Reid, Y. Liu, P. Janscak, et al. 2013. FBH1 helicase disrupts RAD51 filaments in vitro and modulates homologous recombination in mammalian cells. *J. Biol. Chem.* 288:34168–34180. http://dx.doi.org/10.1074/jbc.M113.484493

Sy, S.M., M.S. Huen, and J. Chen. 2009a. MRG15 is a novel PALB2-interacting factor involved in homologous recombination. *J. Biol. Chem.* 284:21127–21131. http://dx.doi.org/10.1074/jbc.C109.023937

Sy, S.M., M.S. Huen, and J. Chen. 2009b. PALB2 is an integral component of the BRCA complex required for homologous recombination repair. *Proc. Natl. Acad. Sci. USA.* 106:7155–7160. http://dx.doi.org/10.1073/pnas.0811159106

Tripathi, V., T. Nagarjuna, and S. Sengupta. 2007. BLM helicase-dependent and -independent roles of 53BP1 during replication stress-mediated homologous recombination. *J. Cell Biol.* 178:9–14. http://dx.doi.org/10.1083/jcb.200610051

Tripathi, V., S. Kaur, and S. Sengupta. 2008. Phosphorylation-dependent interactions of BLM and 53BP1 are required for their anti-recombinogenic roles during homologous recombination. *Carcinogenesis.* 29:52–61. http://dx.doi.org/10.1093/carcin/bgm238

van Brabant, A.J., T. Ye, M. Sanz, J.L. German III, N.A. Ellis, and W.K. Holloman. 2000. Binding and melting of D-loops by the Bloom syndrome helicase. *Biochemistry.* 39:14617–14625. http://dx.doi.org/10.1021/bi0018640

Veaute, X., J. Jeusset, C. Soustelle, S.C. Kowalczykowski, E. Le Cam, and F. Fabre. 2003. The Srs2 helicase prevents recombination by disrupting Rad51 nucleoprotein filaments. *Nature.* 423:309–312. http://dx.doi.org/10.1038/nature01585

Wang, A.T., T. Kim, J.E. Wagner, B.A. Conti, F.P. Lach, A.L. Huang, H. Molina, E.M. Sanborn, H. Zierhut, B.K. Cornes, et al. 2015. A dominant mutation in human RAD51 reveals its function in DNA interstrand crosslink repair independent of homologous recombination. *Mol. Cell.* 59:478–490. http://dx.doi.org/10.1016/j.molcel.2015.07.009

Wang, W., M. Seki, Y. Narita, T. Nakagawa, A. Yoshimura, M. Otsuki, Y. Kawabe, S. Tada, H. Yagi, Y. Ishii, and T. Enomoto. 2003. Functional relation among RecQ family helicases RecQL1, RecQL5, and BLM in cell growth and sister chromatid exchange formation. *Mol. Cell. Biol.* 23:3527–3535. http://dx.doi.org/10.1128/MCB.23.10.3527-3535.2003

Ward, I.M., B. Reina-San-Martin, A. Olaru, K. Minn, K. Tamada, J.S. Lau, M. Cascalho, L. Chen, A. Nussenzweig, F. Livak, et al. 2004. 53BP1 is required for class switch recombination. *J. Cell Biol.* 165:459–464. http://dx.doi.org/10.1083/jcb.200403021

Wu, L., and I.D. Hickson. 2003. The Bloom's syndrome helicase suppresses crossing over during homologous recombination. *Nature.* 426:870–874. http://dx.doi.org/10.1038/nature02253

Wu, L., S.L. Davies, N.C. Levitt, and I.D. Hickson. 2001. Potential role for the BLM helicase in recombinational repair via a conserved interaction with RAD51. *J. Biol. Chem.* 276:19375–19381. http://dx.doi.org/10.1074/jbc.M009471200

Xia, B., Q. Sheng, K. Nakanishi, A. Ohashi, J. Wu, N. Christ, X. Liu, M. Jasin, F.J. Couch, and D.M. Livingston. 2006. Control of BRCA2 cellular and clinical functions by a nuclear partner, PALB2. *Mol. Cell.* 22:719–729. http://dx.doi.org/10.1016/j.molcel.2006.05.022

Xu, X., Z. Weaver, S.P. Linke, C. Li, J. Gotay, X.W. Wang, C.C. Harris, T. Ried, and C.X. Deng. 1999. Centrosome amplification and a defective G2-M cell cycle checkpoint induce genetic instability in BRCA1 exon 11 isoform-deficient cells. *Mol. Cell.* 3:389–395. http://dx.doi.org/10.1016/S1097-2765(00)80466-9

Zhang, F., J. Ma, J. Wu, L. Ye, H. Cai, B. Xia, and X. Yu. 2009. PALB2 links BRCA1 and BRCA2 in the DNA-damage response. *Curr. Biol.* 19:524–529. http://dx.doi.org/10.1016/j.cub.2009.02.018